NASA/TM–2010-216695

Fatigue Crack Closure Analysis Using Digital Image Correlation

William P. Leser
North Carolina State University, Raleigh, North Carolina

John A. Newman
Langley Research Center, Hampton, Virginia

William M. Johnston
Lockheed Martin Engineering and Sciences
Langley Research Center, Hampton, Virginia

May 2010

NASA STI Program . . . in Profile

Since its founding, NASA has been dedicated to the advancement of aeronautics and space science. The NASA scientific and technical information (STI) program plays a key part in helping NASA maintain this important role.

The NASA STI program operates under the auspices of the Agency Chief Information Officer. It collects, organizes, provides for archiving, and disseminates NASA's STI. The NASA STI program provides access to the NASA Aeronautics and Space Database and its public interface, the NASA Technical Report Server, thus providing one of the largest collections of aeronautical and space science STI in the world. Results are published in both non-NASA channels and by NASA in the NASA STI Report Series, which includes the following report types:

- TECHNICAL PUBLICATION. Reports of completed research or a major significant phase of research that present the results of NASA programs and include extensive data or theoretical analysis. Includes compilations of significant scientific and technical data and information deemed to be of continuing reference value. NASA counterpart of peer-reviewed formal professional papers, but having less stringent limitations on manuscript length and extent of graphic presentations.

- TECHNICAL MEMORANDUM. Scientific and technical findings that are preliminary or of specialized interest, e.g., quick release reports, working papers, and bibliographies that contain minimal annotation. Does not contain extensive analysis.

- CONTRACTOR REPORT. Scientific and technical findings by NASA-sponsored contractors and grantees.

- CONFERENCE PUBLICATION. Collected papers from scientific and technical conferences, symposia, seminars, or other meetings sponsored or co-sponsored by NASA.

- SPECIAL PUBLICATION. Scientific, technical, or historical information from NASA programs, projects, and missions, often concerned with subjects having substantial public interest.

- TECHNICAL TRANSLATION. English-language translations of foreign scientific and technical material pertinent to NASA's mission.

Specialized services also include creating custom thesauri, building customized databases, and organizing and publishing research results.

For more information about the NASA STI program, see the following:

- Access the NASA STI program home page at *http://www.sti.nasa.gov*

- E-mail your question via the Internet to help@sti.nasa.gov

- Fax your question to the NASA STI Help Desk at 443-757-5803

- Phone the NASA STI Help Desk at 443-757-5802

- Write to:
  NASA STI Help Desk
  NASA Center for AeroSpace Information
  7115 Standard Drive
  Hanover, MD 21076-1320

NASA/TM–2010-216695

Fatigue Crack Closure Analysis Using Digital Image Correlation

William P. Leser
North Carolina State University, Raleigh, North Carolina

John A. Newman
Langley Research Center, Hampton, Virginia

William M. Johnston
Lockheed Martin Engineering and Sciences
Langley Research Center, Hampton, Virginia

National Aeronautics and
Space Administration

Langley Research Center
Hampton, Virginia 23681-2199

May 2010

The use of trademarks or names of manufacturers in this report is for accurate reporting and does not constitute an official endorsement, either expressed or implied, of such products or manufacturers by the National Aeronautics and Space Administration.

Available from:

NASA Center for AeroSpace Information
7115 Standard Drive
Hanover, MD 21076-1320
443-757-5802

Abstract

Fatigue crack closure during crack growth testing is analyzed in order to evaluate the critieria of ASTM Standard E647 for measurement of fatigue crack growth rates. Of specific concern is remote closure, which occurs away from the crack tip and is a product of the load history during ΔK-reduction fatigue crack growth testing. Crack closure behavior is characterized using relative displacements determined from a series of high-magnification digital images acquired as the crack is loaded. Changes in the relative displacements of features on opposite sides of the crack are used to generate crack closure data as a function of crack wake position. For the results presented in this paper, remote closure did not affect fatigue crack growth rate measurements when ASTM Standard E647 was strictly followed and only became a problem when testing parameters (e.g., load shed rate, initial ΔK, etc.) greatly exceeded the guidelines of the accepted standard.

Introduction

Fatigue crack growth (FCG) test data are most commonly presented in plots of FCG rate (da/dN) as a function of the cyclic crack-tip stress intensity factor, ΔK, herein called the crack driving force. A schematic of a typical FCG rate curve is shown in Figure 1. Using logarithmic axes, typical engineering alloys exhibit a linear FCG-rate-versus-ΔK relation at intermediate ΔK values (Paris regime), with crack growth rates rapidly increasing at higher ΔK values (near the fracture toughness) and with rapidly decreasing rates as a FCG threshold (ΔK_{th}) is approached (ref. 1). The near-threshold region, characterized by slow crack growth rates, is of primary concern to the authors. Accurate determination of ΔK_{th} is of practical importance for life prediction of many components due to the extremely slow FCG rates, and the tendency of the crack driving force, ΔK, to increase with increasing crack length. The majority of fatigue life for many aircraft components is consumed near the threshold and small changes in ΔK_{th} can significantly affect the predicted fatigue life. Therefore, it is important to characterize the crack growth threshold (ΔK_{th}), and understand mechanisms that influence threshold, most notably crack closure, the crack-face contact that occurs during cyclic loading (refs. 2-5).

Naturally-occurring cracks initiate under near-threshold loading conditions and propagate under increasing-ΔK conditions. Development of FCG rate curves is problematic in that test cracks can not be practically started in the threshold region, mimicking service conditions by generating the entire FCG curve under increasing ΔK conditions. For practical reasons, tests are typically started in the Paris regime (intermediate ΔK values) while the applied loads are gradually reduced such that ΔK values decrease as the crack propagates, as indicated by the dashed-red curve in Figure 1. Care must be taken to ensure that this artificial loading does not affect the fatigue crack growth rate data. ASTM standard E647 ("Standard Test Method for Measurement of Fatigue Crack Growth Rates") was developed to ensure satisfactory test results are obtained (ref. 6).

Recent research suggests that performing crack growth tests under ΔK-reduction conditions can adversely affect the FCG data (refs. 7, 8) due to a test-history-induced crack closure phenomenon. During cyclic loading, crack faces can contact before the load reaches the minimum value, a phenomenon called crack closure, which is naturally occurring, and typically occurs near the crack tip (see Figure 2a). However, when crack closure is a product of the load reduction method, such that contact away from the crack tip occurs first (termed "remote closure"; see Figure 2b), the FCG data are affected in an artificial

way, i.e., the results would be a product of the test history and not an indication of the mechanical performance. Here, remote closure is assumed to be a product of high crack-tip plasticity created at high ΔK near the start of the FCG test.

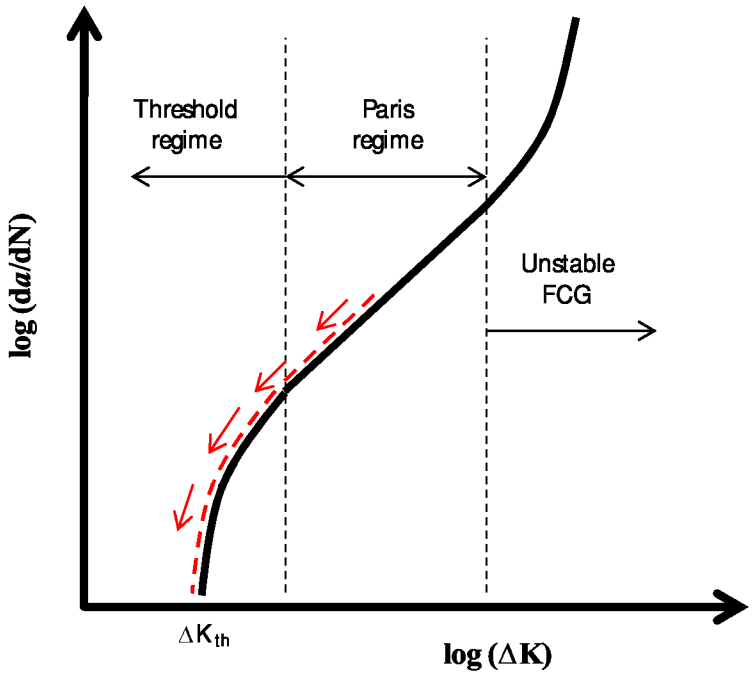

Figure 1. Schematic of a typical FCG rate curve.

Remote closure will likely result in artificially high values of ΔK_{th}, as shown schematically in Figure 3, because the reduction in the crack-tip driving force is a result of the crack-wake load history rather than the mechanical performance of the material. In the absence of remote closure, the FCG threshold would be ΔK_{th1}, but due to remote closure that may develop as a threshold test progresses, a threshold value of ΔK_{th2} is obtained. In this example, if the non-conservative threshold value of ΔK_{th2} is used in the design of a component, premature failure may occur.

Although ASTM standard E647 appears to produce good data for a wide range of materials, it was developed to be material independent. However, the level of crack-tip plasticity and, therefore, the likelihood of remote closure, is dependent on material behavior (e.g., yield stress). Further, a significant practical concern with the standard is that as a test approaches the threshold region, the FCG growth rates become very slow, which requires extensive amounts of machine time. Accelerating the test, especially near the threshold region, would greatly improve testing efficiency if it could be done without sacrificing the quality of the results (i.e., no remote closure). Therefore the objective of this study is to investigate the possibility of exceeding the ASTM standards, using aluminum alloys, without producing remote closure. Ultimately this approach should be used as an experimental approach to obtain an optimized testing procedure.* In this paper, data from FCG tests done, both in accordance with, and in violation of, ASTM Standard E647 will be analyzed to obtain detailed fatigue crack closure profiles to characterize crack closure during the tests.

* Here, optimization means determining the most rapid (in terms of machine time) load history that will achieve FCG threshold conditions without remote closure.

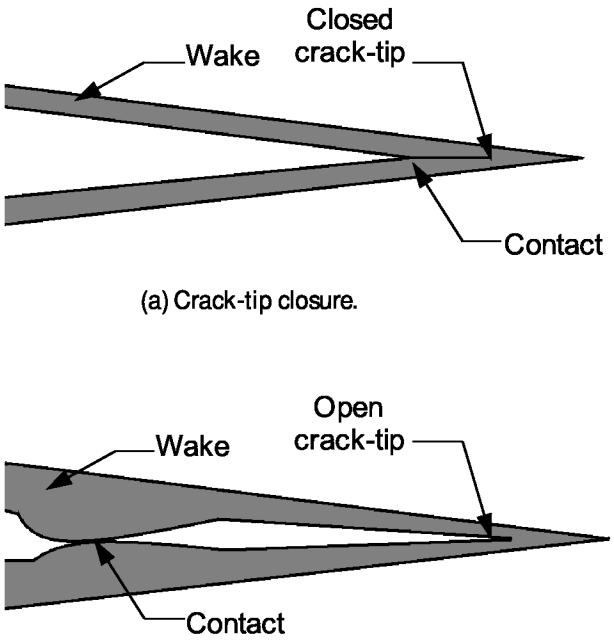

Figure 2. Schematics of fatigue crack closure scenarios: (a) Crack tip closure and (b) Remote closure.

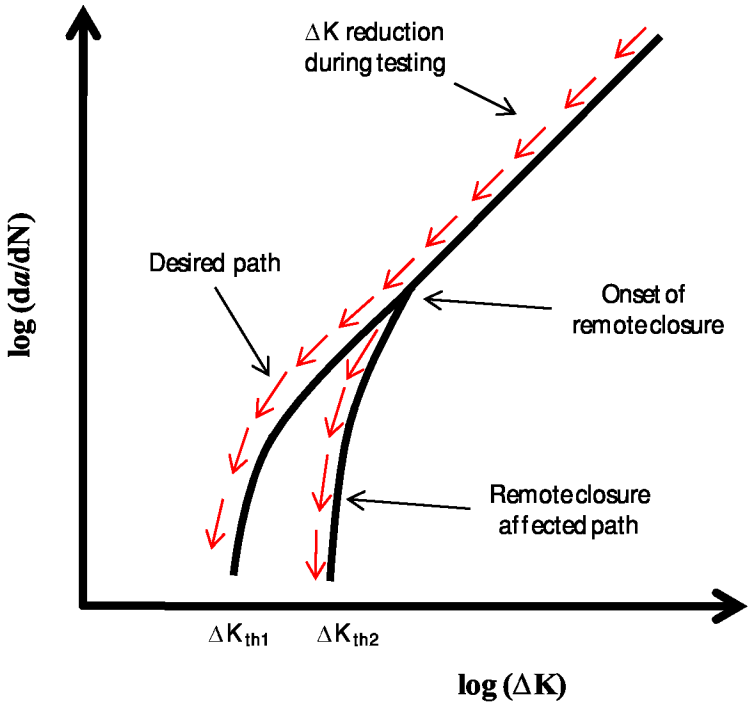

Figure 3. FCG Rate curves illustrating likely changes in ΔK_{th} when remote closure occurs (ΔK_{th2}) and in the absence of remote closure (ΔK_{th1}) (ref. 5).

Testing

Fatigue crack growth tests were performed using closed-loop servo-hydraulic test machines with constant amplitude sinusoidal loading. With only noted exceptions, testing was conducted in accordance with ASTM standard E647 using eccentrically-loaded single-edge notch tension (ESE(T)) specimens (ref. 9) having width, W, and thickness, B, of 38.1 mm and 2.3 mm, respectively. A computer-controlled system (ref. 10) was used to continuously monitor crack length during testing using the back-face compliance technique (ref. 11). This system automatically adjusts loads as the crack grows to ensure that programmed stress intensity factors are applied throughout the tests.

Crack closure data was obtained by analyzing a series of high-magnification (300-700X) images of the crack obtained during cyclic loading. A photograph of the equipment used (microscope, digital camera, and test machine) is shown in Figure 4. A random pattern of 4 μm speckles was deposited on specimen surfaces in the region of crack growth to provide features whose motion can be tracked as a function of load in the digital images. A photograph of a specimen with a field of speckles applied to the surface is shown in Figure 5. At high-magnification (lower portion of Figure 5), individual speckles can be seen. The relative displacement of features on either side of the crack is used to determine when crack closure occurs. The cyclic loading was slowed to 0.01 Hz (one load cycle per 100 seconds) and images were captured every second for more than two complete load cycles (240 total images).

.

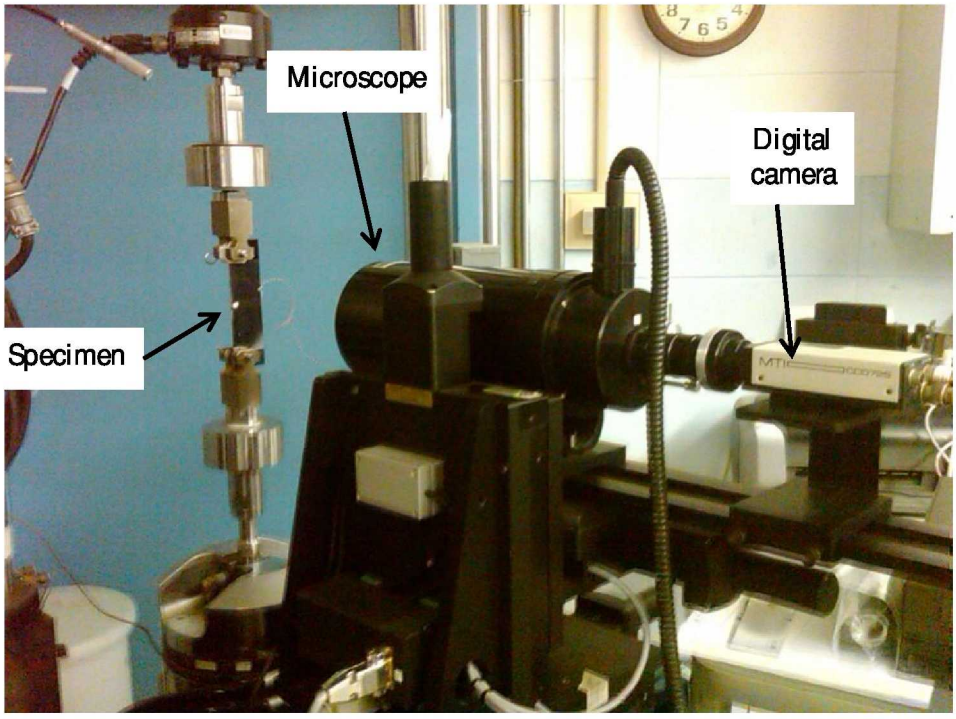

Figure 4. Servo-hydraulic test stand and digital camera with microscope.

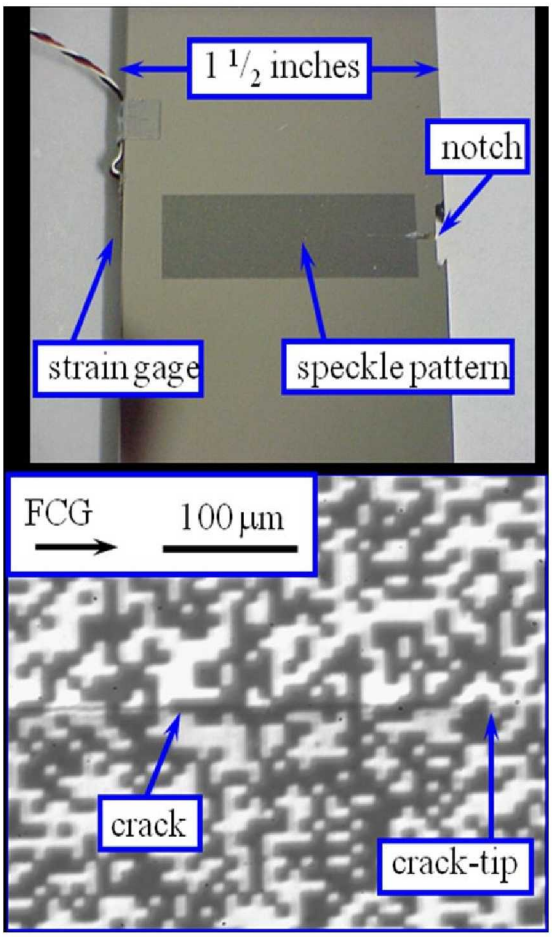

Figure 5: Specimen with speckle pattern.

Digital Image Correlation

The digital image correlation system provides 2D displacement data from the series of pictures taken during the test. The digital images captured during cyclic loading were analyzed using VIC-2D (ref. 12), an image processing program developed by Correlated Solutions, Inc.[†] Digital images of the speckled regions of the specimen were loaded into the image correlation system. An area of interest was selected on the first photograph, which defined the area where displacement data were taken. Over the entire selected area of interest, subsets of pixels are tracked in each image relative to their position in the reference image. This image correlation process results in a series of displacement fields that can be post-processed in order to observe how the strain field changes throughout the load cycle. An example of an image correlation system generated strain field (ε_{yy}, strain in vertical direction) for the wake of a loaded fatigue crack is shown in Figure 6.

[†] Herein, VIC-2D will be referred to as "image correlation system."

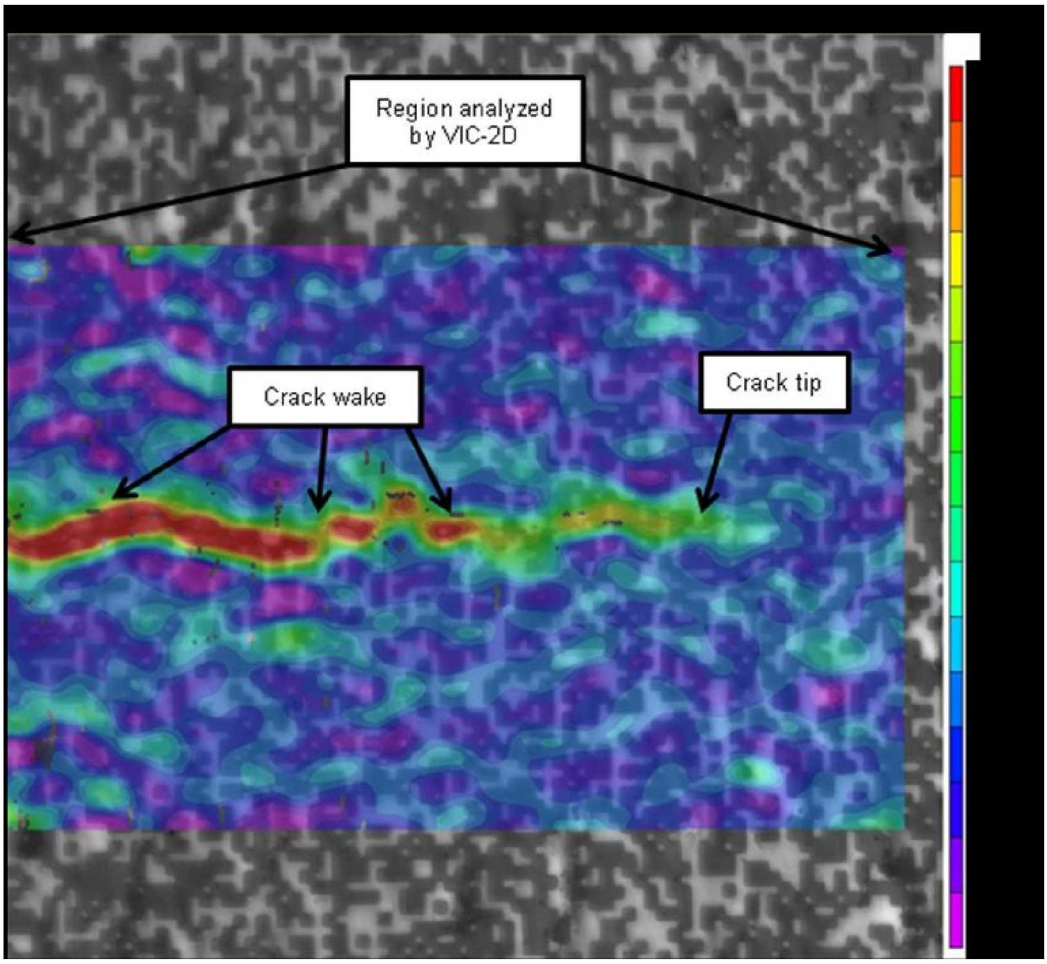

Figure 6. A typical image correlation system generated crack-wake strain field.

Closure Analysis

After the digital images were analyzed using the image correlation system, the displacement data were analyzed using the Elber method to determine the load at which the crack closed (ref. 13). In this method, the crack-opening displacement at a point along the crack wake was plotted against load resulting in a compliance plot for that specific crack-wake location. Deviations in linearity on this plot indicate crack closure. A typical plot of crack opening compliance is shown in Figure 7a. To better determine deviations from linearity, a least squares regression analysis was performed on the closure-free portion of the compliance plot. The error was then calculated between the data points and the regression line. These error values were then plotted against load; this is called a reduced compliance plot. A typical plot of reduced compliance is shown in Figure 7b. Two regression lines were then fit to the reduced compliance data. The first is fit to the data that were assumed to be closure free (in the example of Figure 7b, all points above a load ratio of 0.6). The second is fit to data affected by closure (in this example, all points below a load ratio of approximately 0.3). The intersection of these two fitted lines was used as the load at which crack closure occurs for that specific crack-wake location. This method was repeated every five pixels (approximately 4 μm for the example of Figure 7) along the crack to produce a closure profile along the crack wake as in Figure 7c.

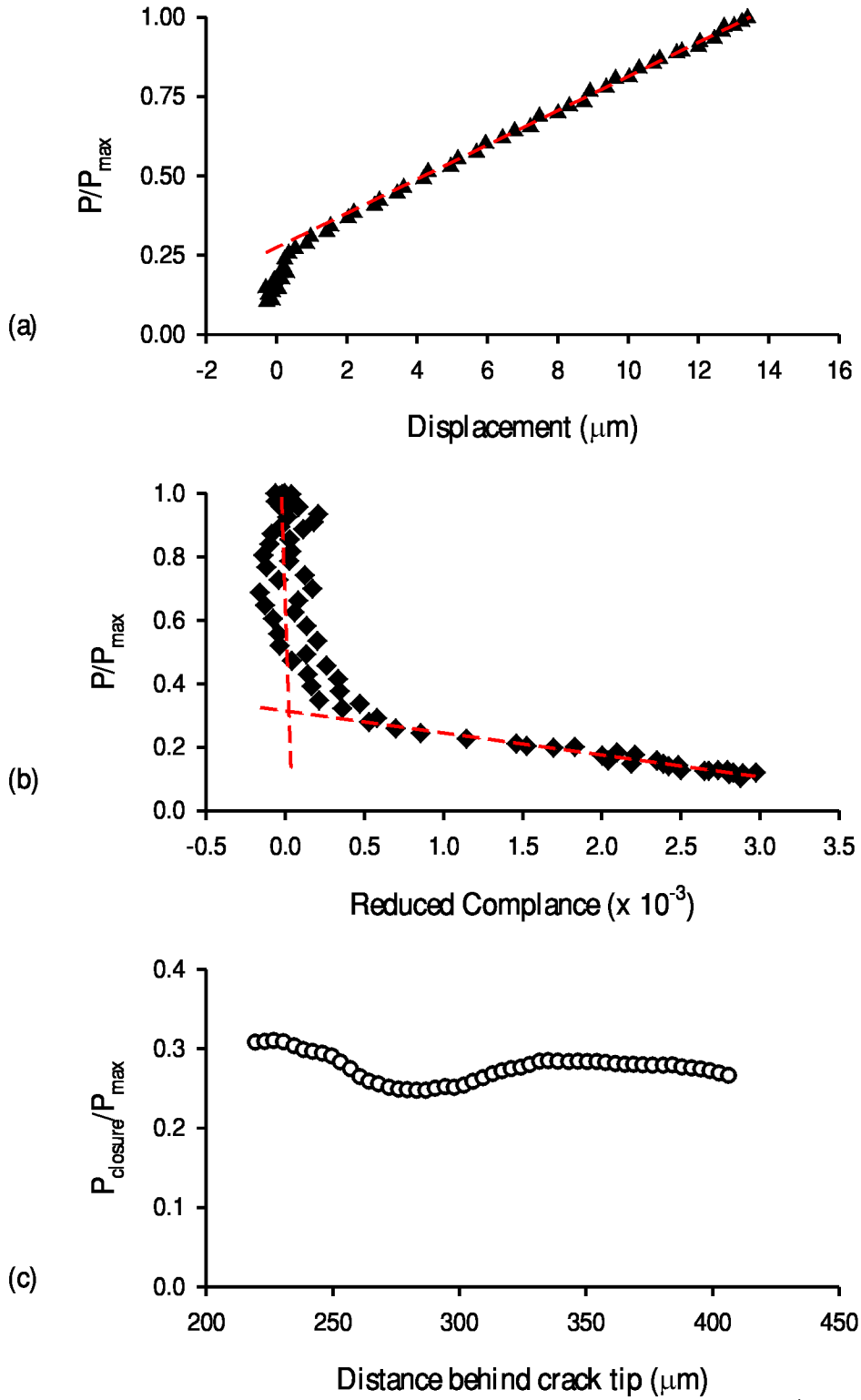

Figure 7. Reduced compliance method as implemented in MATLAB.‡

‡ MATLAB is a registered trademark of The Math Works, Inc.

Results

To validate the image correlation system method, digital images from a test that had been previously analyzed using an older image correlation system were reanalyzed (ref. 5). Here, constant-ΔK fatigue crack growth testing was conducted on an aluminum alloy 8009 specimen at R = 0.05 and K_{max} = 5.5 MPa$\sqrt{m}$ (ΔK = 4.95 MPa$\sqrt{m}$) until steady-state crack growth conditions were achieved. Testing was momentarily stopped while alumina slurry (Al_2O_3 particles mixed with methanol) was introduced in the crack mouth to simulate a thick crack-mouth oxide layer. Fatigue loading resumed and the crack wake was analyzed after 130 μm of crack growth. The results of this previous study are shown in Figure 8 using circular symbols. Crack closure levels in much of the crack wake occur near $R_{contact}$ (ratio of contact load and maximum load) of 0.5, as indicated by the horizontal red dashed line. Closure loads decrease between the location of the crack-wake particles (130 μm from the crack tip) and the crack tip. Closure data obtained from the image correlation system (analyzing the same digital images) are also shown in Figure 8 (solid line curve). These data exhibit nearly the same behavior as the previous results suggesting that the image correlation system is able to reproduce the results from reference 5, but with the advantage of generating data at hundreds of additional crack-wake locations.

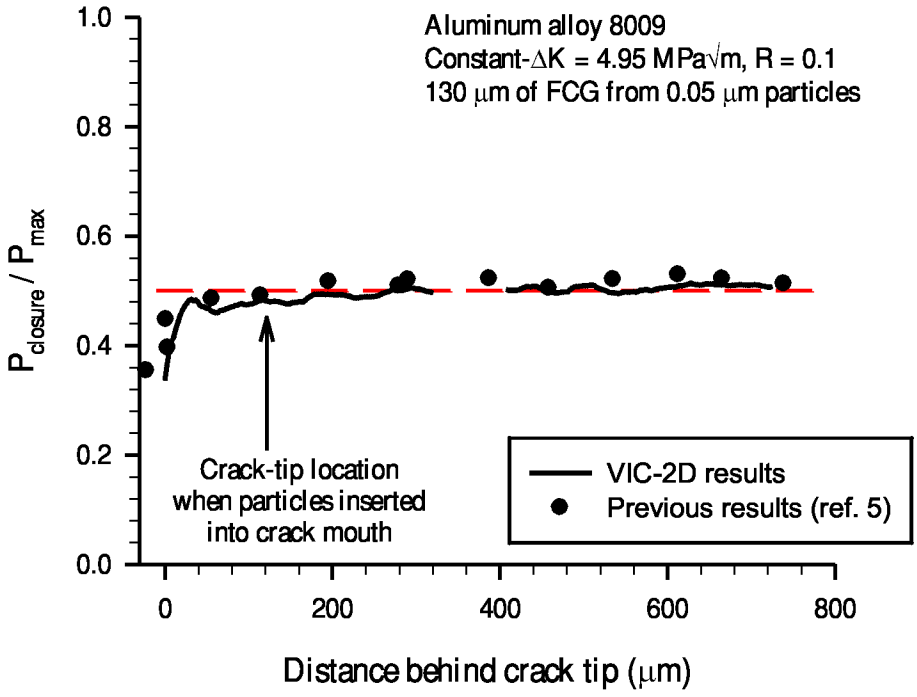

Figure 8. Comparison of image correlation system (VIC-2D) results with published results.

Preliminary results of this study have demonstrated that remote closure can occur when the testing parameters recommended by ASTM Standard E647 are greatly exceeded. Figure 9 shows the closure profile of an aluminum alloy 8009 specimen tested at constant-R = 0.1 conditions (initial K_{max} = 11 MPa$\sqrt{m}$ and C = -393.7/m)[§] obtained using the image correlation system. The experimental results of

[§] The rate of change in ΔK during fatigue crack growth testing is characterized by the K-gradient, C. Negative values indicate that ΔK values decrease as the crack propagates. Standard test methods require C > -78.7/m. See reference 6 for details.

Figure 9 were taken after approximately 3mm of crack growth (ΔK = 3.3 MPa$\sqrt{m}$), which is approaching the R = 0.1 FCG threshold value for this alloy. High-magnification images were taken at three locations; near the crack tip, the location corresponding to the start of the ΔK-reduction test, and further behind the crack tip (corresponding to steady state pre-cracking at ΔK = 9.9 MPa$\sqrt{m}$, R = 0.1). This test exceeds the ASTM standard E647 limits on the K-gradient, C, by a factor of 5. Here, remote closure is shown to occur because crack closure occurs in the crack wake before occurring at the crack tip. The horizontal red dashed line in the figure corresponds to the mean normalized closure load ($P_{closure}/P_{max}$ = 0.21) of the crack wake. In comparison, the crack tip closes later (at a lower load $P_{closure}/P_{max}$ = 0.12), which is the definition of remote closure, and is assumed to be an artifact of the test procedure.

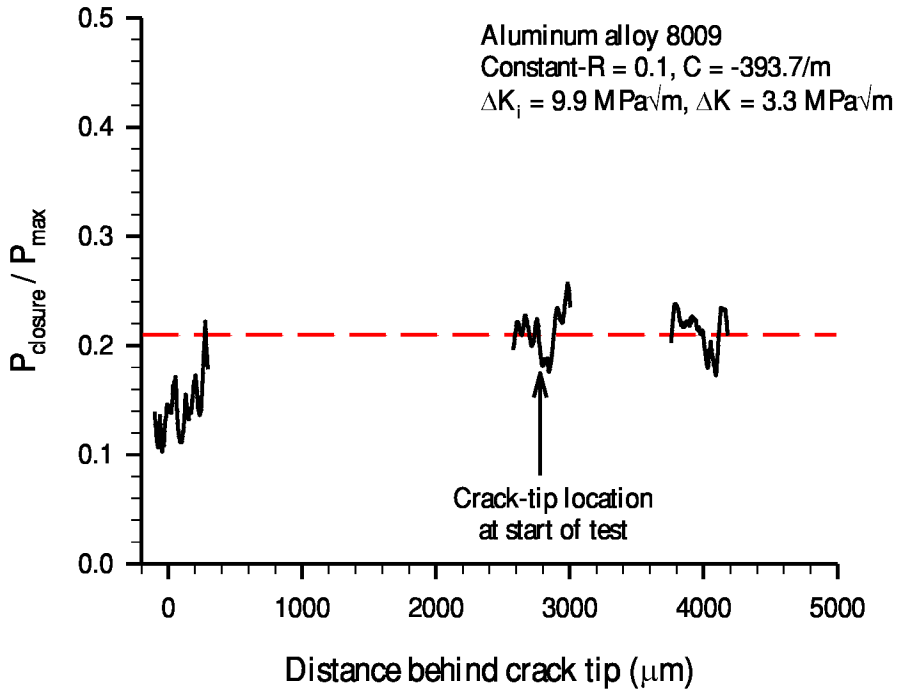

Figure 9. Closure profile for a specimen of aluminum alloy 8009 with initial K_{max} = 11 MPa$\sqrt{m}$ (ΔK_i = 9.9 MPa$\sqrt{m}$) and C = -393.7/m. Remote closure occurs.

However, experimental results also show that the guidelines of ASTM standard E647 are overly-conservative for some load scenarios. Figure 10 shows the closure profile (crack closure loads as a function of distance behind the crack tip) of a specimen of an aluminum alloy 8009 specimen tested at an initial K_{max} = 11 MPa$\sqrt{m}$ and C = -393.7/m. The data presented in Figure 10 correspond to a ΔK = 7.4 MPa$\sqrt{m}$, after 800 μm of crack growth from the start of the test. Here, crack closure occurs in the crack wake at approximately $P_{closure}/P_{max}$ = 0.25, as indicated by the horizontal red dashed line. Closure loads ($P_{closure}/P_{max}$) increase closer to the crack tip (within 100 μm of the crack tip), increasing to approximately $P_{closure}/P_{max}$ = 0.36 at the crack tip. In this case, crack closure occurs first at the crack tip with closure occurring in the crack wake at lower loads, in a manner characteristic of steady-state crack closure in the absence of load history effects (ref. 14).

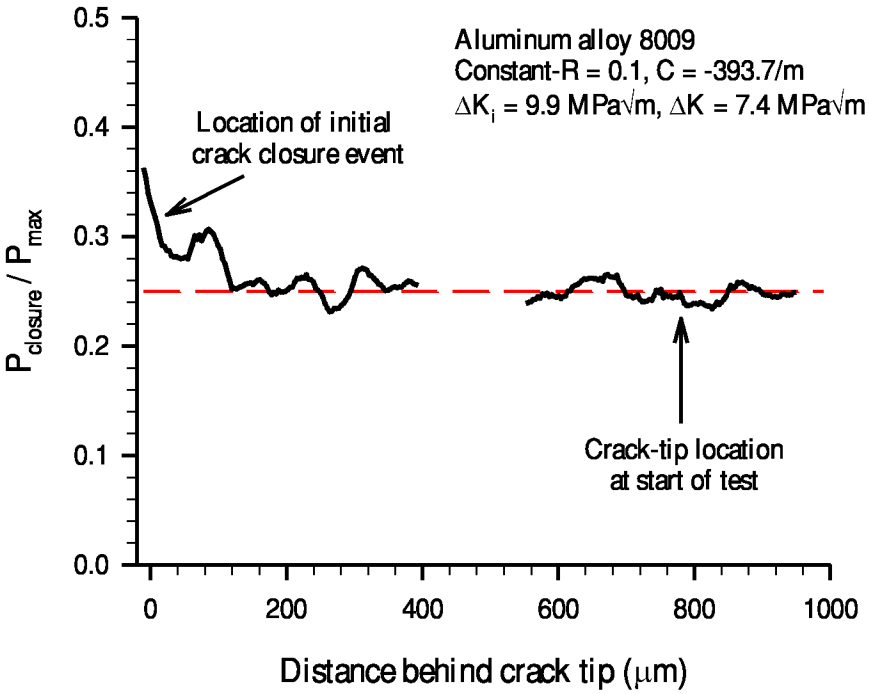

Figure 10. Closure profile for a specimen of aluminum alloy 8009 with initial K_{max} = 11 MPa√m (ΔK_i = 9.9 MPa√m) and C = -393.7/m. No remote closure.

A test with the same conditions as in Figure 10 was conducted on an aluminum alloy 2024 specimen, a material with different crack closure characteristics. These constant-R = 0.1 FCG data are presented in Figure 11 (initial K_{max} = 11 MPa√m and C = -393.7/m). Crack closure data were acquired after approximately 1 mm of crack growth from the start of the test, corresponding to a ΔK = 6.7 MPa√m (nearly the same ΔK value as for the data of Figure 10). Crack closure occurs in the crack wake at approximately $P_{closure}/P_{max}$ = 0.60, as indicated by the horizontal red dashed line. Closure loads ($P_{closure}/P_{max}$) decrease closer to the crack tip (within 100 μm of the crack tip), reaching approximately $P_{closure}/P_{max}$ = 0.3 near the crack tip. Here, the first crack closure event (highest $P_{closure}/P_{max}$) occurs in the crack wake (distance from crack tip > 100 μm) meaning that remote closure occurs, presumably as a product of the load history.

A final example is presented that conforms with ASTM Standard E647. Here, a constant-R = 0.1 FCG test is conducted on an aluminum alloy 7055 specimen (initial ΔK = 5.94 ksi√in, C = -78.7/m). Crack closure data for this test are presented in Figure 12 after approximately 2.5 mm of crack growth (from the start of the ΔK-reduction test), corresponding to an applied ΔK = 4.95 MPa√m. Crack closure in the crack wake, near the start of the test, was determined to be approximately $P_{closure}/P_{max}$ = 0.27. Within 400 μm of the crack tip, closure loads are shown to increase from this value ($P_{closure}/P_{max}$ = 0.27) to approximately $P_{closure}/P_{max}$ = 0.4 near the crack tip. This crack closure profile, characterized by the first closure event occurring near the crack tip with crack-wake locations closing at lower loads, is similar to that shown in Figure 10 and typical behavior of steady-state conditions, i.e., not affected by load history.

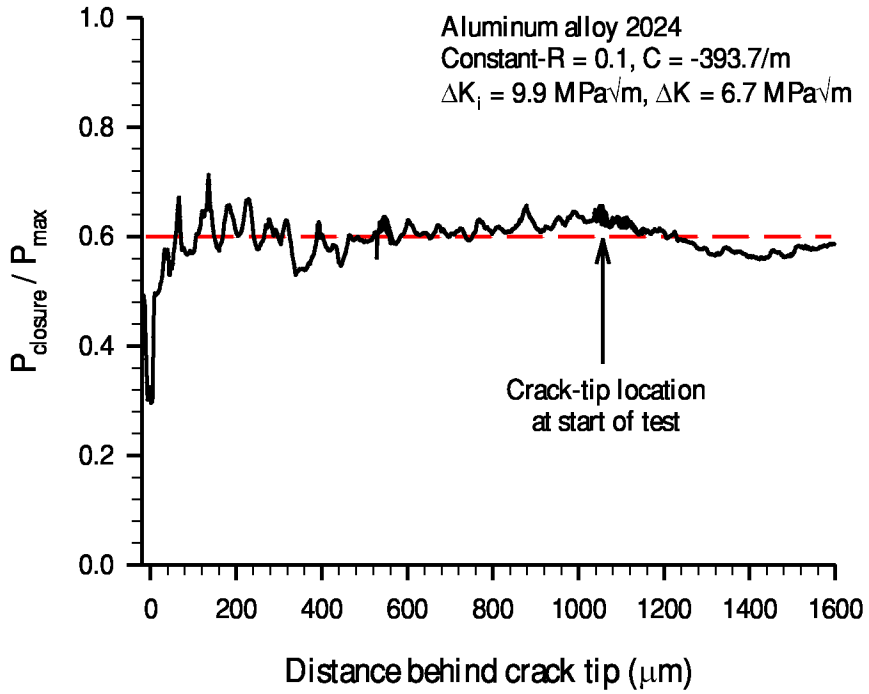

Figure 11. Closure profile for a specimen of aluminum alloy 2024 with initial K_{max} = 11 MPa√m (ΔK_i = 9.9 MPa√m) and C = -393.7/m. Remote closure occurs.

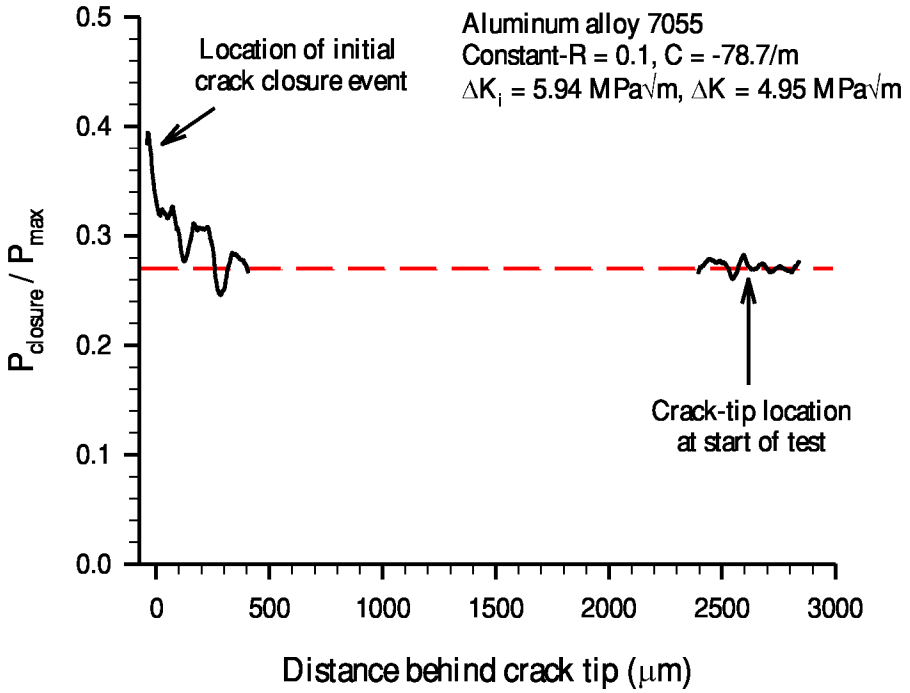

Figure 12. Crack closure profile for aluminum alloy 7055 with initial K_{max} = 6.6 MPa√m (ΔK_i = 5.94 MPa√m) and C = -78.7/m. Remote closure does not occur.

Discussion of Results

Digital image analysis (VIC-2D) has been used to characterize crack closure along the wake of a propagating crack during constant-R ΔK-reduction testing. Although unnatural (meaning that this is not a load history typical of service cracks), generating FCG data using this test method is practical as long as the load history does not affect the resulting FCG test results. Despite some studies that suggest following ASTM Standard E647 can result in remote closure and artificially-high values of ΔK_{th} (refs. 7, 8), the results presented in this paper suggest otherwise. Two examples were shown (recall Figures 10 and 12) where the ΔK-reduction test did not result in remote closure, despite the fact that in one case (Figure 10) the ASTM criterion on the K-gradient ($C \geq -78.7/m$) was violated by a factor of 5. Therefore, the results presented in this paper suggest that the ΔK-reduction testing prescribed by ASTM standard E647 is not only capable of producing good data (meaning not affected by remote closure), but is likely overly conservative in that tests may be able to operate at faster ΔK-shed rates without producing remote-closure-affected data. Further study is needed to determine an optimal load history.**

An optimal load history for ΔK-reduction testing will likely be material dependent. Consider the difference in the observed crack closure characteristics between Figures 10 and 11, despite being subjected to nearly identical load histories. In this case, the most significant difference between these tests is the alloys. The tests corresponding to Figures 10 and 11 were performed on aluminum alloys 8009 and 2024, respectively. Aluminum alloy 8009 is a very fine-grained (typical grain diameter approximately 0.5 μm) powder-metallurgy alloy having an elastic modulus and yield stress of 87.6 GPa and 419.9 MPa, respectively (refs. 15-17). Aluminum alloy 2024 has a relatively coarse microstructure (typical grain size 70-150 μm) and has elastic modulus and yield stress of 71.7 GPa and 350.3 MPa, respectively (refs. 18, 19). Although these alloys have similar tensile properties, the fine-grain alloy (8009) was free of remote closure while the coarse-grain alloy (2024) was affected by remote closure, at least for the test conditions associated with Figures 10 and 11. Differences in crack-path roughness might be a factor, but additional study is needed before conclusions can be made.

Summary

This research has shown that remote closure may occur, especially when the criteria of ASTM standard E647 are violated. However, results presented in this paper suggest that the current standard is overly conservative for some test and material combinations such that the criteria of ASTM E647 can be violated without inducing remote closure. Any procedure for optimized load shedding (allow most rapid load shedding without sacrificing data integrity) should consider specific material properties, but more research is needed to determine which material properties are important.

Acknowledgement

The work described in this paper was conducted while one author (W.P. Leser) was a Langley Aerospace Research Summer Scholar (LARSS) student in residence at NASA Langley Research Center during the summer of 2009.

** Here, optimal means the fastest ΔK-reduction test that does not result in remote closure.

References

1. P.C. Paris and F. Erdogan, "A Critical Analysis of Crack Propagation Laws," *Journal of Basic Engineering*, Transactions of the ASME, Dec. 1963, pp. 528-534.

2. W. Elber, "Fatigue Crack Closure Under Cyclic Tension," Engineering Fracture Mechanics, Volume 2, 1970, pp. 37-45.

3. J. A. Newman, and R. S. Piascik, "Plasticity and Roughness Closure Interactions Near the Fatigue Crack Growth Threshold," Fatigue and Fracture Mechanics: 33rd Volume, ASTM STP 1417, W. G. Reuter and R. S. Piascik, Eds., ASTM International, West Conshohocken, PA, 2002.

4. S. Suresh, *Fatigue of Materials*, Cambridge University Press, 1991, Cambridge, UK.

5. J. A. Newman, The Effects of Load Ratio on Threshold Fatigue Crack Growth of Aluminum Alloys, Ph.D. dissertation, 2000, Virginia Polytechnic Institute and State University.

6. ASTM Standard E647 "Standard Test Method for Measurement of Fatigue Crack Growth Rates."

7. J.C. Newman, Jr. and Y. Yamada, "Compression Precracking Methods to Generate Near-threshold Fatigue-crack growth-rate Data," *International Journal of Fatigue*, in press as of August 2009.

8. S.C. Forth, J. C. Newman, Jr., and R.G. Forman, "On Generating Fatigue Crack Growth Thresholds," *International Journal of Fatigue*, Vol. 25, 2003, pp. 9-15.

9. R.S. Piascik, J.C. Newman, Jr., and J. H. Underwood, "The Extended Compact Tension Specimen," *Fatigue and Fracture of Engineering Materials and Structures*, Vol. 20, 1997, pp. 559-563.

10. Fracture Technology Associates, *8VHU¶V 5HIHUHQFH 0DQXDO IRU $XWRPDWHG)DWLJXH &UDFN *URZWK* Version 2.43, Fracture Technology Associates, Bethlehem, PA.

11. W.F. Deans, C.B. Jolly, W.A. Poyton, and W. Watson, "A Strain Gauging Technique for Monitoring Fracture Specimens During Environmental Testing," *Strain*, Vol. 13, 1977, pp. 152-154.

12. M.A. Sutton, J.-J. Orteu, and H.W. Schreier, *Image Correlation for Shape, Motion and Deformation Measurements*, Springer Science Business Media, New York, NY, 2009.

13. W. Elber, "Crack Closure and Crack Growth Measurements in Surface-Flawed Titanium Alloy Ti-6Al-4V," 1975, NASA TN-D-8010.

14. W.T. Riddell and R.S. Piascik, "Stress Ratio Effects on Crack Opening Loads and Crack Growth Rates in Aluminum Alloy 2024," NASA/TM-1998-206929.

15. A.P. Reynolds, "Constant Amplitude and Post-Overload Fatigue Crack Growth Behavior in PM Aluminum Alloy AA 8009," *Fatigue and Fracture of Engineering Materials and Stuctures*, Vol. 15, 1992, pp. 551-562.

16. G.H. Bray, A.P. Reynolds, and E.A. Starke, Jr., "Mechanisms of Fatigue Crack Growth Retardation Following Single Overloads in Powder Metallurgy Aluminum Alloys," *Metallurgical Transactions*, Vol. 23A, 1992, pp. 3055-3066.

17. W.C. Porr and R.P. Gangloff, "Elevated Temperature Fracture of RS/PM Alloy 8009: Part I. Fracture Mechanics Behavior," *Metallurgical and Materials Transactions*, Vol. 25A, 1994, pp. 365-379.

18. J.E. Hatch, Editor, *Aluminum: Properties and Physical Metallurgy*, American Society for Metals, Metals Park, OH, 1984.

19. J.R. Davis, Editor, *Aluminum and Aluminum Alloys*, ASM International, 1993.

REPORT DOCUMENTATION PAGE

Form Approved
OMB No. 0704-0188

The public reporting burden for this collection of information is estimated to average 1 hour per response, including the time for reviewing instructions, searching existing data sources, gathering and maintaining the data needed, and completing and reviewing the collection of information. Send comments regarding this burden estimate or any other aspect of this collection of information, including suggestions for reducing this burden, to Department of Defense, Washington Headquarters Services, Directorate for Information Operations and Reports (0704-0188), 1215 Jefferson Davis Highway, Suite 1204, Arlington, VA 22202-4302. Respondents should be aware that notwithstanding any other provision of law, no person shall be subject to any penalty for failing to comply with a collection of information if it does not display a currently valid OMB control number.
PLEASE DO NOT RETURN YOUR FORM TO THE ABOVE ADDRESS.

1. REPORT DATE *(DD-MM-YYYY)*	2. REPORT TYPE	3. DATES COVERED *(From - To)*
01-05-2010	Technical Memorandum	

4. TITLE AND SUBTITLE
Fatique Crack Closure Analysis Using Digital Image Correlation

5a. CONTRACT NUMBER

5b. GRANT NUMBER

5c. PROGRAM ELEMENT NUMBER

6. AUTHOR(S)
Leser, William P.; Newman, John A.; Johnston, William M.

5d. PROJECT NUMBER

5e. TASK NUMBER

5f. WORK UNIT NUMBER
645846.02.07.07.03.01

7. PERFORMING ORGANIZATION NAME(S) AND ADDRESS(ES)
NASA Langley Research Center
Hampton, VA 23681-2199

8. PERFORMING ORGANIZATION REPORT NUMBER
L-19865

9. SPONSORING/MONITORING AGENCY NAME(S) AND ADDRESS(ES)
National Aeronautics and Space Administration
Washington, DC 20546-0001

10. SPONSOR/MONITOR'S ACRONYM(S)
NASA

11. SPONSOR/MONITOR'S REPORT NUMBER(S)
NASA/TM-2010-216695

12. DISTRIBUTION/AVAILABILITY STATEMENT
Unclassified - Unlimited
Subject Category 26
Availability: NASA CASI (443) 757-5802

13. SUPPLEMENTARY NOTES

14. ABSTRACT
Fatigue crack closure during crack growth testing is analyzed in order to evaluate the critieria of ASTM Standard E647 for measurement of fatigue crack growth rates. Of specific concern is remote closure, which occurs away from the crack tip and is a product of the load history during crack-driving-force-reduction fatigue crack growth testing. Crack closure behavior is characterized using relative displacements determined from a series of high-magnification digital images acquired as the crack is loaded. Changes in the relative displacements of features on opposite sides of the crack are used to generate crack closure data as a function of crack wake position. For the results presented in this paper, remote closure did not affect fatigue crack growth rate measurements when ASTM Standard E647 was strictly followed and only became a problem when testing parameters (e.g., load shed rate, initial crack driving force, etc.) greatly exceeded the guidelines of the accepted standard.

15. SUBJECT TERMS
Crack closure; Fatigue crack growth testing; Load history

16. SECURITY CLASSIFICATION OF:			17. LIMITATION OF ABSTRACT	18. NUMBER OF PAGES	19a. NAME OF RESPONSIBLE PERSON
a. REPORT	b. ABSTRACT	c. THIS PAGE			STI Help Desk (email: help@sti.nasa.gov)
					19b. TELEPHONE NUMBER *(Include area code)*
U	U	U	UU	19	(443) 757-5802